The Structures of Complexes between Polyethylene Imine and Sodium Dodecyl Sulfate in D_2O: A Scattering Study

L. A. Bastardo,*,†,‡ V. M. Garamus,§ M. Bergström,†,‡,⊥ and P. M. Claesson†,‡

Department of Chemistry, Surface Chemistry, Drottning Kristinas väg 51, Royal Institute of Technology, SE-10044 Stockholm, Sweden, YKI, Institute for Surface Chemistry, Box 5607, SE-11486, Stockholm, Sweden, and GKSS Research Centre, Max-Plank Strasse, 21502 Geesthacht, Germany

Received: July 16, 2004; In Final Form: October 11, 2004

The association between a highly branched polyelectrolyte with ionizable groups, polyethylene imine (PEI), and an anionic surfactant, sodium dodecyl sulfate (SDS), has been investigated at two pH values, using small-angle neutron and light scattering. The scattering data allow us to obtain a detailed picture of the association structures formed. Small-angle neutron scattering (SANS) measurements in solutions containing highly charged PEI at low pH and low SDS concentrations indicate the presence of disklike aggregates. The aggregates change to a more complex three-dimensional structure with increasing surfactant concentration. One pronounced feature in the scattering curves is the presence of a Bragg-like peak at high q-values observed at a surfactant concentration of 4.2 mM and above. This scattering feature is attributed to the formation of a common well-ordered PEI/SDS structure, in analogue to what has been reported for other polyelectrolyte−surfactant systems. Precipitation occurred at the charge neutralization point, and X-ray diffraction measurements on the precipitate confirmed the existence of an ordered structure within the PEI/SDS aggregates, which was identified as a lamellar internal organization. Polyethylene imine has a low charge density in alkaline solutions. At pH 10.1 and under conditions where the surfactant was contrast matched, the SANS scattering curves showed only small changes with increasing surfactant concentration. This suggests that the polymer acts as a template onto which the surfactant molecules aggregate. Data from both static light scattering and SANS recorded under conditions where SDS and to a lower degree PEI contribute to the scattering were found to be consistent with a structure of stacked elliptic bilayers. These structures increased in size and became more compact as the surfactant concentration was increased up to the charge neutralization point.

Introduction

Polyethylene imine (PEI) is a hyperbranched polyelectrolyte that has been extensively used in a range of applications, including cosmetics (e.g. in antiperspirants and hair conditioners), as a wet strength agent in the paper industry, flocculating agent of silicate soils in mining, and in gene delivery therapy, just to mention a few.[1−4] This polyelectrolyte is highly charged at low pH, but its charge density decreases as the pH is increased.[5,6]

The interactions between PEI and sodium dodecyl sulfate (SDS) have been investigated in some detail. Some of these studies report unusual behavior of the PEI/SDS system.[4,5,7−10] For instance, conductivity changes for low charged hyperbranched PEI, and for polyvinylamine, mixed with SDS were reported by Bystryak et al.[6] Here an increase in the PEI−SDS solution conductivity, compared to the conductivity of pure surfactant solution, was observed. These changes in conductivity values were accompanied by an increase in the solution pH due to consumption of hydrogen ions by the PEI/SDS complex. However, the increased hydroxide ion concentration was not sufficient to explain the surprisingly high conductivity of PEI/SDS solutions at high pH. Later Winnik et al.[10] suggested that a high mobility of charged species within the PEI/SDS aggregates was the reason for the high conductivity, but no detailed picture of the internal organization of the aggregates was offered.

Another investigation focused on association between PEI and SDS at different pH values.[5] At low surfactant concentration, the SDS ions bind in a monomer form, and at this stage the PEI/SDS complex forms a thermodynamically stable solution. Above a critical SDS concentration the aggregates precipitate, and thus the dispersion becomes thermodynamically unstable. The rate of precipitation was found to be dependent on the method of preparation. This reflects the fact that strongly associating polymer−surfactant systems are prone to be trapped in long-lived nonequilibrium states.[11]

SANS, among other techniques, has been used to study the complexes formed between SDS and uncharged ethoxylated PEI.[8] For most of the samples studied by SANS, bound micelles to the polyelectrolyte were detected. However, these results cannot be used for drawing conclusions about the association structures formed by nonethoxylated PEI and SDS.

The association between PEI and SDS at the solid−liquid interface at pH 5.5−6 has also been investigated[12] by using surface force techniques, AFM, and ESCA. PEI was preadsorbed on negatively charged muscovite mica and found to adsorb in a flat conformation on the surface. The PEI adsorption caused a strong recharging, in agreement with previous studies.[13−15] Due to the positive net charge of the surface, SDS was found

* Corresponding author. E-mail: luis.bastardo@surfchem.kth.se.
† Royal Institute of Technology.
‡ YKI, Institute for Surface Chemistry.
§ GKSS Research Centre.
⊥ Present address: Department of Pharmacy, Pharmaceutical Physical Chemistry, Uppsala University, Box 580, SE-751 23 Uppsala, Sweden.

10.1021/jp046837o CCC: $30.25
Published on Web 12/07/2004

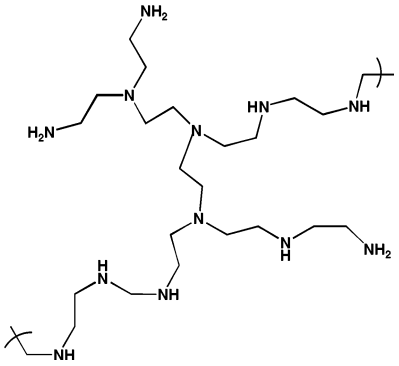

Figure 1. A typical structural element of polyethylene imine.

to associate with the PEI layer at very low concentrations, resulting in close to charge neutralization. However, at higher SDS concentrations, about 0.5 cmc, additional SDS was adsorbed, mainly in a bilayer that was formed on top of the PEI layer.

Sum frequency vibrational spectroscopy has been used to study the influence of PEI on the adsorption of SDS at the solid/liquid interface. [16] The samples were prepared at pH 6. From here, it was concluded that the association between surfactant and polyelectrolyte was primarily electrostatically driven. Both the conformational order and the packing density of the SDS on the PEI increased with the surfactant concentration. A certain degree of cooperativity in the SDS/PEI interaction in addition to the electrostatic interaction is believed to be the driving force for the formation of an ordered layer of surfactant on the polyelectrolyte.

Even though a considerable amount of work has been done to understand the association between PEI and SDS, there is as yet no clear picture of the structures formed due to PEI−SDS association, and how these structures evolve as a result of changing the surfactant concentration and pH value. In this report we describe results obtained using scattering of light, neutrons, and X-rays that allow us to probe different length scales. As a result we are able to draw rather detailed conclusions about the structures formed by PEI−SDS association at both low and high pH values.

Materials and Methods

Materials. Polyethylene imine, PEI, was obtained from Polyscience in the form of a 30 wt % aqueous solution. A typical structural element, containing primary, secondary, and tertiary amines in the ratio 1:2:1, is shown in Figure 1. The polyelectrolyte was used as received. Sodium dodecyl sulfate was obtained from Sigma (lot no. 129110002), and deuterated sodium dodecyl sulfate (SDS-*d*) was provided by Cambridge Laboratories. Both surfactants were used as received. D_2O was chosen as solvent to minimize the incoherent background from hydrogen and obtain a high scattering contrast in the SANS measurements. The pH of some of the solutions was lowered by adding a small amount of DCl (obtained as a 35% solution in D_2O from Cambridge laboratories).

Stock solutions of a relatively high concentration of PEI were prepared in D_2O around 12 h in advance of starting the measurements. The solutions were diluted with D_2O to the desired concentration just prior to starting the experiments. When studying mixtures of SDS and PEI, the stock polymer solution was always added to the surfactant solution to a final concentration of 2000 ppm. It is important to point out that when measuring the hydrogen ion activity in deuterated solutions with the usual pH cell, the values should be corrected by using the classical pD scale at 25 °C,[17,18] with improvements made by Krezel et al.:[19]

$$\mathrm{pD} = 0.929\ \mathrm{pH\ meter\ reading} + 0.42 \qquad (1)$$

Static Light scattering (SLS). Static light scattering experiments were performed with a light scattering equipment from Brookhaven consisting of a BI-200SM goniometer and a BI-9000AT digital autocorrelator. An argon ion laser (Lexel laser, model 95-2) operating at 514 nm wavelength and emitting vertically polarized light was used as a light source. The measurements were done at 26 different angles in the range of $20° \le \theta \le 150°$, corresponding to q values in the range of 5.67×10^{-4}Å $\le q \le 31.5 \times 10^{-4}$Å. For each angle five different measurements were performed and subsequently averaged. The data were normalized to absolute scale by using toluene as a reference.[20,21] The average molecular weights and the second virial coefficient were calculated via a conventional Zimm plot, where the reciprocal intensity of the scattered light ($1/\Delta R(\Theta,c)$) was plotted versus q^2, according to the equation:

$$\frac{4\pi^2 n_o^2 (\mathrm{d}n/\mathrm{d}c)^2}{N_A \lambda_o^4} \frac{c}{\Delta R(\Theta,c)} = \left[\frac{1}{M_w}\right]\left[1 + \left(\frac{R_g q^2}{3}\right) + 2A_o c\right] \qquad (2)$$

where n_o is the refractive index of the solvent (1.33); dn/dc is the refractive index increment of the solution (0.2432 cm^3/g for PEI at pD 10.1 and 0.2998 cm^3/g for PEI at pD 4.9, determined with an interferometric refractometer: Optilab DSP from Wyatt technology); c is the polymer concentration, which was varied from 1000 to 5000 ppm at both pD values; N_A is Avogadro's number; M_w is the weight average molecular weight; q is the scattering wave vector; A_o is the second virial coefficient; and R_g the radius of gyration.

Each fit to constant angle data is extrapolated to zero concentration, and each fit at constant concentration is extrapolated to zero angle, obtaining two lines. The average molecular weight (M_w) is calculated from the intercept of each extrapolated line with the y-axis. R_g is calculated from the slope of the extrapolated line at zero concentration, and the second virial coefficient (A_o) is calculated from the slope of the extrapolated line at zero angle. All solutions were prepared in D_2O, and no salt was added. The temperature was 25 °C.

Dynamic Light Scattering (DLS). The DLS measurements were performed with the light scattering equipment from Brookhaven described above. In all cases the scattered light was measured at an angle of 90° relative to the primary bean. The second-order cumulant expansion and the CONTIN methods were used to analyze the measured autocorrelation functions. These methods are described in detail in refs 22 and 23, respectively.

Small-Angle Neutron Scattering. The SANS experiments were performed at the SANS1 instrument at the FRG1 research reactor at GKSS Research Centre, Geesthacht, Germany.[24] A range of scattering vectors ($0.005 < q < 0.25$ Å^{-1}) was obtained by using three sample-to-detector distances (0.7−9.7 m). The neutron wavelength was 8.1 Å, and the wavelength resolution was 10% (full width at half-maximum value). The samples were kept at 25 ± 0.5 °C in quartz cuvettes with a path length of 1 or 2 mm. The raw SANS spectra were corrected for background from the solvent, sample cell, and other sources by conventional procedures.[25] The two-dimensional isotropic scattering spectra were azimuthally averaged, converted to an absolute scale, and corrected for detector efficiency by dividing by the incoherent

scattering spectrum of pure water,[26] which was measured with a 1 mm path length quartz cell.

The relevant excess scattering length density per unit mass of solute for the measurements were $\Delta\rho$ SDS-d/D_2O = 0.3 × 10^{11} m/Kg, $\Delta\rho$ SDS-h/D_2O = −5.14 × 10^{11} m/Kg, and $\Delta\rho$ PEI/D_2O = −3.09 × 10^{11} m/Kg; note that the hydrogen atoms bound to the amine groups in PEI become exchanged for deuterium in D_2O.[27] The value for $\Delta\rho$ PEI/D_2O above was calculated for uncharged PEI. The corresponding value for fully charged PEI is −2.7 × 10^{11} m/Kg. At pD 4.9 and 10.1, the degree of ionization is 65% and about 11%, respectively.[5]

The SLS data were multiplied by the following factor to convert it into "neutron units":

$$\frac{K_C}{K_{SLS}}\frac{(\Delta\rho)^2}{N_A} \tag{3}$$

where

$$K_{SLS} = \frac{4\pi^2 n_o{}^2 (dn/dc)^2}{N_A \lambda_o{}^4} \text{ and } K_C = \frac{32 \times 10^{-6}}{I_{tol}}\left(\frac{n_o}{n_{tol}}\right)^2 \tag{4}$$

$\Delta\rho$ is the scattering length density per unit mass of the sample calculated as:

$$(\Delta\rho) = X_{pol}\Delta\rho_{pol} + X_{suf}\Delta\rho_{surf} \tag{5}$$

here X_{pol} and X_{surf} are the mass fraction of the polymer and surfactant in the sample, respectively, while $\Delta\rho_{pol}$ and $\Delta\rho_{surf}$ are the scattering length densities of the PEI and SDS, respectively (see values above).

I_{tol} is the scattering intensity value for toluene and n_{tol} is the refractive index for toluene (1.4712). [28]

X-ray Diffraction. The X-ray diffraction experiments were performed on the X-ray diffractometer XRD 3003 PTS (Seifert & Co, Germany). The X-ray line used was Cu Kα (λ = 1.54 Å). The range of measured angles was up to 12° (0.046 Å^{-1} < q < 0.85 Å^{-1}). The pinhole geometry was chosen for the measurements. The sample holder was made from a glass capillary with diameter 1 mm. The temperature of the sample was 25 °C.

Scattering Data Analysis. A combination of SANS and SLS data for each sample containing PEI and SDS at pD 10.1 in D_2O could be fitted with a model for elongated bilayers ordered in 1-dimensional stacks. Accordingly, the scattering cross-section per unit mass of solid can be written as

$$\frac{d\sigma(q)}{d\Omega} = \Delta\rho_m{}^2 \langle M\rangle_w P_{bil}(q) P_{ell}(q) Z(q) \tag{6}$$

where $\Delta\rho_m$ is the difference in scattering length per unit mass of solute between particles and solvent and $\langle M\rangle_w$ is the weight-average molar mass. The form factor is here separated into one contribution that accounts for the cross-section of a planar bilayer

$$P_{bil}(q) = \left(\frac{\sin(q\xi)}{q\xi}\right)^2 \tag{7}$$

and the form factor of an infinitely thin elliptical disk with half axis a and b

$$P_{ell}(q) = \frac{2}{\pi}\int_0^{\pi/2} \frac{2[1 - B_1(2qr(a,b,\phi))/qr(a,b,\phi)]}{(qr(a,b,\phi))^2}\, d\phi \tag{8}$$

where $r(a,b,\phi) = \sqrt{a^2\sin^2\phi + b^2\cos^2\phi}$.

TABLE 1: Summary of Static Light Scattering Results for PEI in D_2O

	R_g (nm)	mol wt	2nd virial coeff (cm^3 mol/g^2)
pD 10.1 fresh	50	7.3 × 10^5	1.2 × 10^{-4}
pD 10.1 24 h old	55	7.6 × 10^5	1.3 × 10^{-4}
pD 4.9 fresh	60	1.2 × 10^6	1.7 × 10^{-4}
pD 4.9 24 h old	60	1.2 × 10^6	1.7 × 10^{-4}

The interference effects of particles ordered in a 1-dimensional array were taken into account with the factor

$$Z(q) = \frac{1 - w^2}{1 + w^2 - 2w\cos(q\langle D\rangle)} \tag{9}$$

in a paracrystal model[29−31] where the average distance between two adjacent particles $\langle D\rangle$ and a relative standard deviation $P \equiv \sigma_D/\langle D\rangle$ of the Gaussian layer distance distribution $w = \exp[-\sigma_D{}^2 q^2/2]$ has been included in the factor.

Throughout the SANS data analysis corrections were made for instrumental smearing.[32,33] For each instrumental setting the ideal model scattering curves were smeared by the appropriate resolution function when the model scattering intensity was compared with the measured one by means of least-squares methods. The parameters in the model were optimized by means of conventional least-squares analysis.[34]

Results

Light Scattering. *Polyethylene Imine with No Added Surfactant.* The results from static light scattering with use of conventional Zimm plots for PEI solutions in D_2O at pD 10.1 are shown in Table 1. Both the weight average molecular weight and the radius of gyration are largely unaffected by allowing the samples to stand for 24 h at room temperature. The second virial coefficient is positive and thus shows that the pair interaction between the polyelectrolytes is repulsive, as expected.[35] We note that the charge density of PEI increases with decreasing pD, and thus the second virial coefficient is higher for samples prepared at lower pD values due to the increased electrostatic repulsion between the polyelectrolytes. The radius of gyration is also found to be higher at the lower pD value, about 60 nm at pD 4.9, as compared to 50−55 nm at pD 10.1. This is consistent with the higher electrostatic repulsion within the polyelectrolyte at lower pD values. The molecular weight of the PEI is found to be higher at pD 4.9 (1.2 × 10^6 g/mol) as compared to that at pD 10.1 (about 7.3 × 10^5 g/mol) by a factor of 1.6. This is not unreasonable considering that an increasing number of chloride ions are associated with the polyelectrolyte at lower pD values. The charged segments making up the structural unit, shown in Figure 1, are $CH_2CH_2ND_3{}^+Cl^-$, $CH_2CH_2ND_2{}^+Cl^-$, and $CH_2CH_2ND^+Cl^-$, and they have a molecular weight that is a factor of about 1.8 higher than that of the uncharged segments $CH_2CH_2ND_2$, CH_2CH_2ND, and CH_2CH_2N, which falls within the difference in molecular weight observed at the two pD values. It should be remembered that the measured value of molecular weight using static light scattering includes the polyion plus a proportional amount of the counterions.[36]

We note that dynamic light scattering measurements of PEI at pD 4.9 and 10.1 show essentially a monomodal but rather broad size distribution (see Figure 2). Hence, it appears that no large PEI aggregates are present, in contrast to what often has been reported for polyelectrolytes in dilute electrolyte solutions, including PEI.[10,37,38] Thus, we conclude that aggregation at pD 4.9 is not the cause of the higher molecular weight observed at

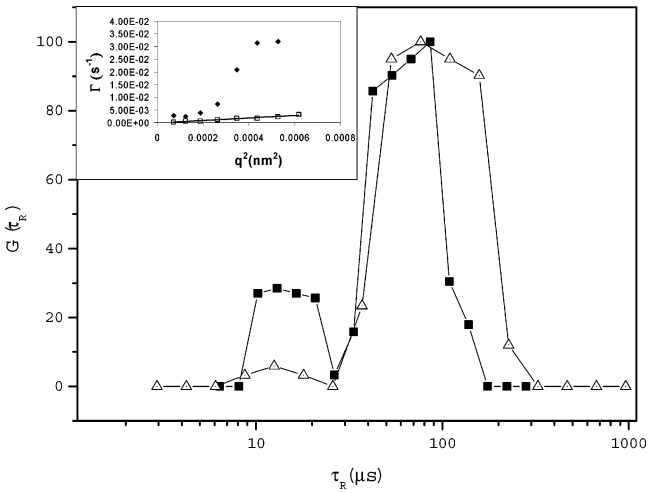

Figure 2. Relaxation time distribution through inverse Laplace transformation of dynamic light scattering data for pure PEI, 2000 ppm at (■) pD 10.1 and (△) pD 4.9. The inset shows Γ ($1/\tau$) as a function of q^2 for PEI at pD 10.1. The intensity for the slow mode (□) increases linearly with q^2, which is indicative of a diffusive motion. On the other hand, the fast mode (♦) does not show a linear dependence of q^2, demonstrating that it is due to internal motions. The same trend for the two modes was also observed for the sample at pD 4.9 (not shown).

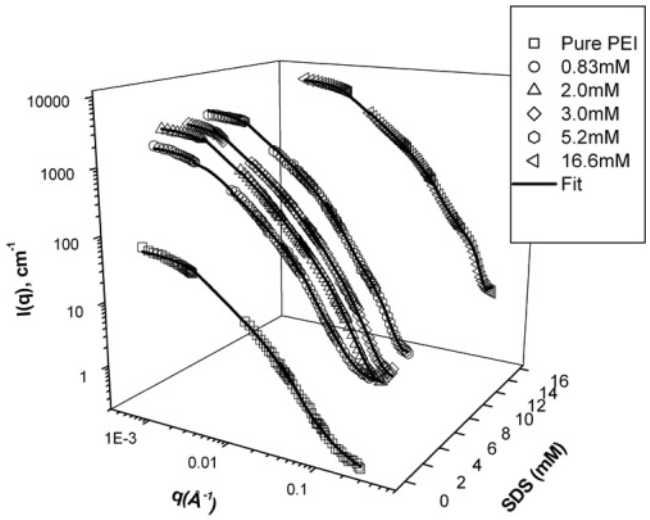

Figure 3. Scattering data for PEI samples (2000 ppm) at pD 10.1 and different SDS-*h* concentrations in D_2O obtained by SANS (high q values) and SLS (low q values). The legends to the right show the SDS-*h* concentration in the samples. The solid lines are calculated scattering curves obtained by using the Paracrystal Ellipsoidal bilayer model as described in the text.

this pD value as compared to that at pD 10.1. We also note that the small peak observed at low relaxation times is not due to diffusion but rather internal motions as evidenced from the nonlinear dependence of the peak intensity when plotted as a function of q^2 (see inset of Figure 2).

Polyethylene Imine Mixed with SDS at pD 10.1. In alkaline solution, pD 10.1, no precipitation of the sample was observed at any surfactant concentration studied, and all solutions were thus clear. This is in good agreement with previous reports on the colloidal stability of PEI−SDS complexes formed at high pH, which showed that the coagulation rate is very slow when there are no inorganic electrolytes present. [5] The static light scattering data for PEI and SDS at pD 10.1 are shown, together with SANS data (Figure 3). Addition of SDS to the PEI solution results in increased scattering up to the highest concentration studied, 16.6 mM (about 2 cmc). However, the shape of the static light scattering curves remains approximately the same.

To obtain an understanding for the association between PEI and the surfactant, as well as the accompanying effect on the scattering curve, the theoretical charge neutralization point was calculated by using the data from ref 5. In our case we had 2000 ppm PEI in the solutions (molecular weight of the EI_{group} was 43.07), with approximately 11% of charged groups[5] at pD 10.1. By using these data, the concentration of charged ethylene imine groups is found to be 5.1 mM.

Assuming that the free SDS concentration is negligible, charge neutralization is expected to occur at this total SDS concentration. However, this is not strictly correct and the free SDS concentration can be estimated from the binding isotherm of Mészáros et al.[5] to be 0.2 mM. As a result the total SDS concentration (i.e. bound + free SDS) at the charge neutralization point could be expected to be 5.3 mM. However, the degree of ionization of PEI increases due to binding of SDS,[5,10] which shifts the charge neutralization concentration to a somewhat higher value. Further, the incorporation of SDS in the aggregates does not stop at the charge neutralization point, but electrophoretic mobility measurements have shown that PEI−SDS aggregates in solutions containing excess SDS have a net negative charge,[12] due to incorporation of excess SDS. Thus, the increase in scattering observed when increasing the SDS concentration from 5.2 to 16.6 mM is due to additional SDS incorporation in the aggregates.

Polyethylene Imine Mixed with SDS at pD 4.9. PEI is highly charged at low pH values, and the degree of ionization at pD 4.9 is about 65%.[5] Neglecting the free SDS concentration results in an expected charge neutralization point at a total SDS concentration of 30.2 mM. The higher charge of PEI at lower pD values results in a stronger electrostatic interaction between the polymer and the surfactant molecules.

The samples were found to be too turbid to allow light scattering measurements at concentrations above 0.83 mM SDS, which shows that the surfactants and the polymer form large aggregates[5,8,38] already at this low surfactant concentration. At higher surfactant concentrations the aggregates precipitate, and they do not redissolve again even at the highest surfactant concentration studied (232 mM). In fact, difficulties with dissolving precipitates formed by highly charged polyelectrolytes and surfactants are commonly observed (see, e.g., refs 39−41).

Small-Angle Neutron Scattering. *Polyethylene Imine Mixed with SDS at pD 10.1.* The scattering curves obtained when the surfactant is contrast matched (SDS-*d* in D_2O), Figure 4, have a low intensity since the (partly deuterated) polyelectrolyte is strongly hydrated and does not form a compact object. The scattering curve without any added SDS can be fitted by using an elongated ellipsoidal structure with half axis dimensions 1100 × 55 × 7 Å^3. Thus, surprisingly, the hyperbranched PEI is highly extended in one direction. Upon addition of SDS, the shape of the scattering curve remains similar but we note a slight increase in the slope of the scatting curve at intermediate q values, indicating a slight compaction of the polyelectrolyte structure. However, there are no major conformational changes of PEI as a result of association with SDS in the surfactant concentration interval investigated, 0−5.2 mM and 16.6 mM. Data obtained with SDS-*h* show, however, that association between surfactant molecules and PEI occurs already at low surfactant concentrations. Since this does not give rise to any significant change in the polymer conformation, the polymer can be viewed as a template where the surfactant molecules adsorb. This is strikingly different compared to association

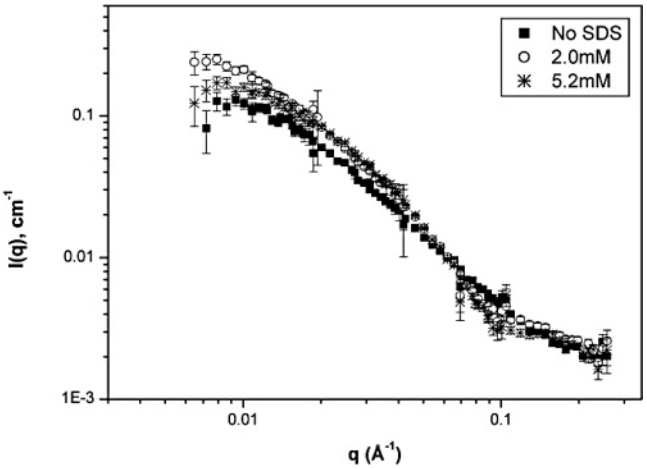

Figure 4. SANS data for PEI samples (2000 ppm) at pD 10.1 and different SDS-*d* concentrations in D_2O. The legends to the right show the SDS-*d* concentration in the samples.

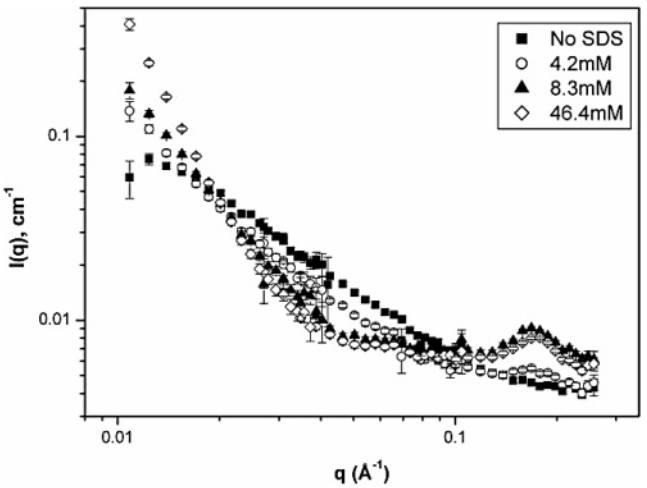

Figure 5. SANS data of PEI samples (2000 ppm) at pD 4.9 and different SDS-*d* concentrations in D_2O. The legends to the right show the SDS-*d* concentration in the samples.

between linear polyelectrolytes and SDS where the association gives rise to significant changes in the polyelectrolyte conformation. Finally we note that scattering curves measured at an SDS concentration of 8.3 mM were not reproducible (data not shown), but in all cases resulted in higher scattering intensity at low *q* values. This is indicative of formation of larger aggregates.

Scattering curves for mixtures of PEI and protonated SDS (SDS-*h*) in D_2O are dominated by scattering from the surfactants (compare Figures 3 and 4). In this case we note a significant increase in the scattering with increasing surfactant concentration (see Figure 3). The shapes of the scattering curves, particularly at higher SDS concentrations, are rather complex showing distinctly different slopes at different *q* ranges. It is, however, possible to reproduce the scattering curves by using appropriate models as will be discussed below.

Polyethylene Imine Mixed with SDS at pD 4.9. Results for the deuterated surfactant samples at pD 4.9 are displayed in Figure 5. As in the pD 10.1 case, the intensity of the scattering curves is quite low. However, we note that the slope of the scattering curve is lower at the lower pD value, which indicates a more extended conformation of the molecules (Figure 6). Addition of SDS to a concentration of 0.4 mM does not result in any significant change in the scattering curve. However, at higher SDS concentrations (4.2 to 46.4 mM) pronounced

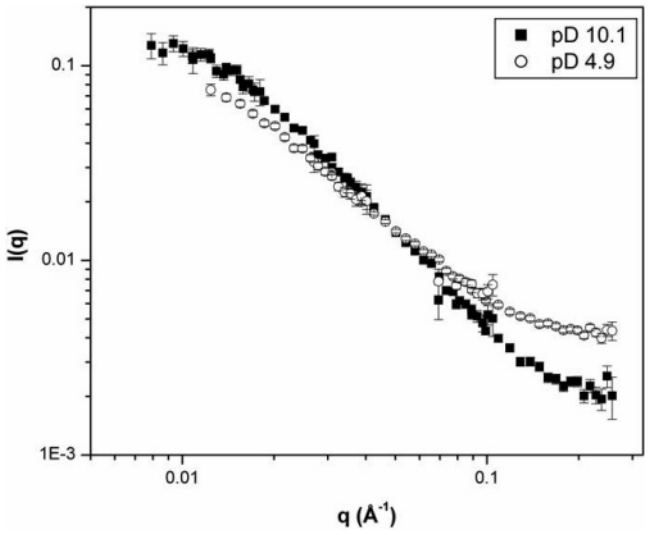

Figure 6. SANS data for D_2O solutions containing PEI (2000 ppm). The legends to the right show the pD values of the samples.

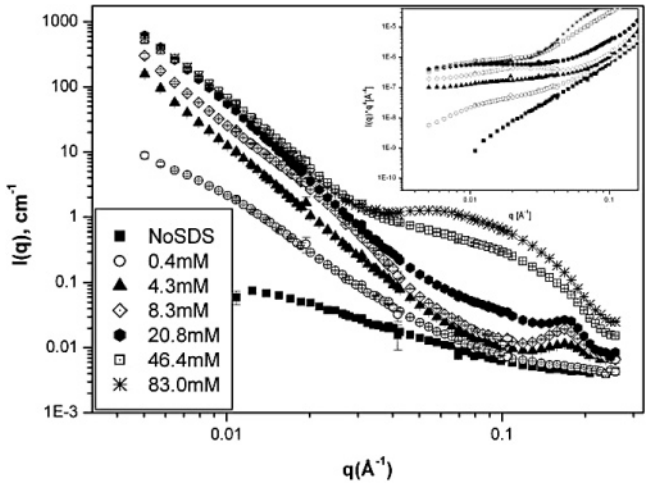

Figure 7. SANS data for PEI samples (2000 ppm) at pD 4.9 and different SDS-*h* concentrations in D_2O. The legends to the left show the SDS-*h* concentration in the samples. The inset shows a plot of $I(q)q^4$ as a function of *q*. At high SDS concentrations the value of Iq^4 becomes close to constant at low *q* values indicative of the presence of large aggregates with sharp interfaces.

changes are observed. The scattering at low *q* values increases, indicating formation of larger aggregates, whereas the scattering at intermediate *q* values decreases. Further, a Bragg-like peak is observed at *q* values around 0.17 $Å^{-1}$, at SDS-*d* concentrations of 4.2 mM and higher. This peak, which corresponds to a repeat distance of 37 Å, is also present when using SDS-*h* (see Figure 7), and thus indicates a common polymer−surfactant structure.[42] Further information on the internal structures of these large PEI−SDS aggregates are obtained by using X-ray diffraction measurements (see below). As in the case of light-scattering measurements, SANS measurements of solutions containing PEI and SDS at pD 4.9 reveal stronger interactions than at high pD.

The data shown in Figure 7, obtained for PEI and SDS-*h* in D_2O, are dominated by the scattering from the surfactants. In this case even very low surfactant additions result in considerable changes in the intensity and the shape of the scattering curve, demonstrating that SDS associates with PEI. The scattering curves obtained at and above an SDS concentration of 8.3 mM show a q^{-4} dependence at low *q* values, demonstrating formation of large three-dimensional aggregates with sharp interfaces. The Bragg-like peak at $q = 0.17$ $Å^{-1}$ is clearly seen

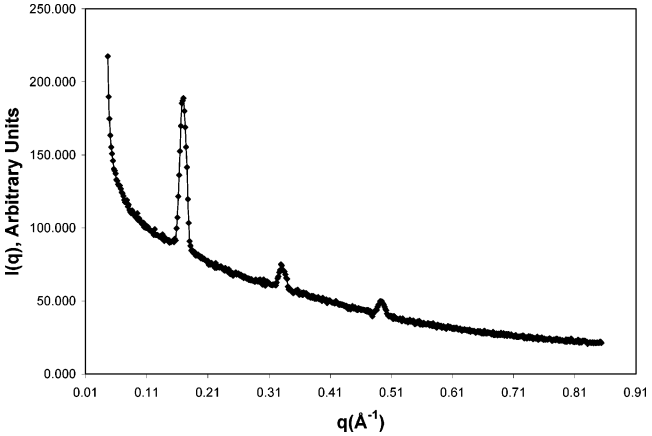

Figure 8. X-ray reflectivity data for a PEI/SDS precipitate in contact with excess solvent. The sample was taken from a sample containing 2000 ppm PEI and 46.4 mM SDS at pD 4.9.

for the samples in the SDS concentration interval 4.3−20.8 mM. This peak is invisible at higher surfactant concentrations due to the strong scattering contribution from free SDS micelles, which gives rise to the broad scattering peak observed for these samples.[43] Note that this does not mean that the ordered PEI−SDS structure is destroyed in excess SDS, but only that it is overwhelmed by the scattering from free micelles in this q range. In fact, the Bragg-like peak is observed also in excess SDS when the surfactant is contrast matched (see Figure 5, which shows that the internal organization persists also in the presence of excess SDS). (Note, we reject that the broad scattering peak observed at high SDS concentrations is due to SDS micelles bound to the PEI since the SDS concentration is well above that needed to fully neutralize the polymer, and due to the observation that the ordered structure giving rise to the Bragg-like peak persists at these high SDS concentrations (see Figure 5).)

X-ray Diffraction. Some precipitate was extracted from a sample above the theoretical charge neutralization point for the PEI samples at pD 4.9 (at a SDS concentration of 46.4 mM). The precipitate, together with some solution, was placed in a glass capillary tube for SAXS analysis. The SAXS profile is shown in Figure 8 and displays three distinct peaks at q values of 0.17, 0.33, and 0.49 Å^{-1}, respectively. The relative positions of the peaks demonstrate that the precipitate has an internal lamellar organization.[44,45]

For stacks of lamellar sheets ordered on top of each other the peaks are located at[44]

$$q_h = \frac{2\pi}{d_h} = \frac{2\pi h}{a} \qquad (2)$$

where a is the distance between two lamellae and $h = 1, 2, 3$, etc. From the data in Figure 8, the repeat distance is calculated to be 37 Å. We suggest that the structural elements are surfactant bilayers separated by PEI. Since the thickness of the hydrocarbon part of an SDS bilayer is of the order of 28 Å, the surfactant headgroup, the polyelectrolyte, and the accompanying water have a thickness of only about 9 Å. Of course, the hydrocarbon part of the surfactant may be somewhat tilted that would increase the water layer thickness, but nevertheless the aqueous compartments within the aggregates are thin, of the order of 10 Å. We note that similar water-poor precipitates have been found to form in other polyelectrolyte−surfactant systems.[44,46]

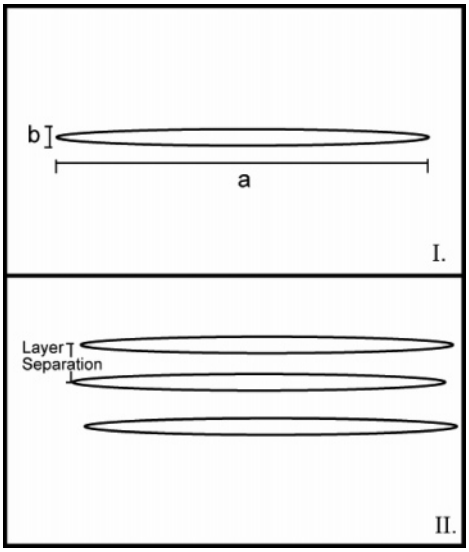

Figure 9. Schematic representation of the model used to fit the SANS data of (I) pure PEI and PEI SDS at low surfactant concentration and (II) PEI/SDS aggregates at higher surfactant concentrations, above 2 mM. Note that the layer separation decreases and becomes more well-defined as the surfactant concentration is increased, but not as well-defined as in the lamellar structure found at lower pD values.

Discussion

The Structure of PEI/SDS Aggregates at pD 10.1. A rather detailed picture of the structure of the PEI/SDS aggregates at pD 10.1 could be obtained by carrying out model fittings to the data obtained by using static light scattering and SANS. To facilitate the fitting the SANS and SLS data were renormalized and put on the same intensity scale as described in the Materials and Methods section.

The scattering curves for samples with high surfactant content were rather complicated with a shoulder at large q values (0.1−0.2 Å^{-1}). Attempts to fit the scattering curves with simple models, such as spherical, rodlike, or disklike objects, failed. However, a model consistent with the scattering form the samples was eventually found. With no or low surfactant addition the scattering curves were found to be consistent with elongated ellipsoids. This model, however, could not explain the data at higher surfactant concentrations, particularly not the pronounced shoulder at high q values. This feature could be reproduced only by including a paracrystal structure factor in the model invoking the stacking of the ellipsoidal aggregates (see Figure 9). We note that this structure shows similarities to the much more ordered lamellar organization found at low pD values, and thus seems to be a logical description of the structural change that occurs as a result of reducing the charge density of the polyelectrolyte.

The scattering curves including the best fit with the model outlined above are shown in Figure 3. The results are quite convincing considering the good fit over the whole q range explored with SLS and SANS. The fitting parameters used for all the samples are summarized in Tables 2 and 3. Table 2 reports the structure of each individual layer and Table 3 describes the overall structure of the stacked layers. First, we note that no stacking of the ellipsoidal aggregates needs to be invoked until the SDS concentration is increased above 0.8 mM (the first concentration above this point was 2 mM). Nevertheless, the molecular mass of the aggregates formed in 0.8 mM SDS solution is significantly higher than that found for the polyelectrolyte alone. The molecular mass increases further with increasing SDS concentration, and the stacked structure clearly

TABLE 2: Dimensions of PEI and Individual PEI/SDS Complexes Calculated from the Fitting Parameters[a]

SDS (mM)	cylinder radius (Å)	half bilayer thickness (Å)	ellipticity	*a* (Å)	*b* (Å)	*V* (Å^3)
0.0	250	7	20	1100	55	1.3×10^6
0.8	210	11	19	900	48	1.5×10^6
2.0	290	12	14	1100	78	3.3×10^6
3.0	250	11	15	960	65	2.2×10^6
5.2	250	13	15	960	64	2.6×10^6
16.6	270	14	23	1300	56	3.2×10^6

[a] The ellipsoid half axes *a* and *b* were calculated from the fitting parameters, which were cylinder radius $= \sqrt{a \cdot b}$ and ellipticity $= a/b$.

TABLE 3: Structural Features Characterizing the Overall Aggregates Formed by PEI and SDS at PD 10.1[a]

SDS (mM)	molecular mass (Mg/mol)	layer separation (Å)	rel layer separation
0.0	0.1[b]		
0.8	1.4		
2.0	4.6	66	0.73
3.0	3.9	56	0.82
5.2	7.3	31	0.68
16.6	33	32	0.39

[a] The values were obtained by fitting SANS and static light scattering data, using eq 6 [b] The fit at low *q*-values was in this case not very accurate and the molecular weight given here is an underestimate. The data in Table 1 is in this respect more accurate.

contains several polyelectrolytes. Considering the constancy of the structure of each layer, Table 2, it appears that each layer consists of one polyelectrolyte with associated SDS.

Once the SDS and PEI start to form stacked structures, an increase in the surfactant concentration leads to a reduction of the layer separation, which is suggested to be due to a decreased electrostatic repulsion and possibly an increased attraction between surfactant tails on neighboring ellipsoidal objects in the stacked structure. We note that the layer separation is not increased again in excess SDS solutions. The relative layer separation is also decreased with increasing surfactant concentration, which means that the distance between the stacked objects becomes better defined.

It is important to emphasize that the size of the individual elliptical PEI/SDS objects remains approximately the same at all surfactant concentrations (see Table 2). The values in the table demonstrate that the axis of the polymer ellipses remains relatively constant at different SDS concentrations, and the variation with SDS concentration is largely attributed to the uncertainties of the fitting process. This confirms that PEI acts as a template for surfactant adsorption and also indicates that each ellipsoidal object consists of one individual PEI molecule with associated SDS molecules. Thus, the association between PEI and SDS at pD 10.1 does not lead to large conformational changes of the polyelectrolyte, but induces a stacking of PEI/SDS complexes in larger aggregates.

The unusual increase in conductivity with addition of SDS to alkaline PEI solutions as reported by Winnik and co-workers[10] was suggested by the authors to be due to a rapid transport of charged species within the aggregates. The aggregate structure deduced from SANS and SLS in this report, consisting of stacked ellipsoidal PEI/SDS complexes, may well provide the means for this charge transport. Surfactant ions could easily be seen to move from one such complex to another through the thin aqueous compartment separating them. The charge-regulating properties of PEI may also be beneficial in this respect since the motion of one SDS molecule from one site on PEI to another would stimulate the removal of the positive charge at the initial binding site and creation of a new positive charge at the final binding site. Thus, the removal and up-take of protons by water in the vicinity of the PEI/SDS complex is suggested to be important for the rapid charge transport within the aggregates.

The Structure of PEI/SDS Aggregates at pD 4.9. The affinity between PEI and SDS is higher at pD 4.9 than under alkaline conditions due to the higher charge density of the polyelectrolyte. The initial binding of SDS does not result in any changes in the scattering curve, but as the association proceeds the polyelectrolytes start to aggregate into larger structures, as evidenced by the change in scattering intensity at intermediate and small *q* values for samples where the surfactant is contrast matched (see Figure 5). We also noted that at 4.2 mM of surfactant the solution was cloudy and the presence of some large aggregates suspended in the solution was evident to the naked eye. These characteristics were observed up to the highest surfactant concentration studied (SDS-*d* 46.4 mM).

For samples where the scattering was dominated by the surfactant (Figure 7), it is clear that the slopes of the curves at intermediate *q* values change from q^{-2} (typical for disk like aggregates),[47] for the lowest surfactant concentration (0.42 mM), to q^{-4}, which is indicative of three-dimensional aggregates with sharp interfaces for concentrations of 4.2 mM SDS and above. It thus seems that the initial stage of association involves binding of surfactants to individual PEI molecules without any large changes of the conformation of the polyelectrolyte itself. Further association results in formation of large three-dimensional aggregates containing several polyelectrolyte chains and SDS. Noticeably, the internal organization of these complexes is well-defined and a Bragg-like peak is a pronounced feature at *q* values around 0.17 Å^{-1}, which corresponds to a repeat distance within these structures of around 37 Å. This value is close to those reported for other highly charged polyelectrolyte−surfactant systems.[42] The fact that the position of the peak is not changed as the surfactant concentration is increased, whereas the intensity increases, demonstrates that a larger fraction of the polyelectrolyte chains adopt the preferred structure as the charge neutralization is approached. A consequence of this is that prior to charge neutralization the surfactants are unevenly distributed among and/or along the polyelectrolyte chains.[42] It also implies that the internal region of the aggregates, where the ordered structure presumably is found, is close to charge neutralized. The excess charges are thus expected to be located at the aggregate surface. X-ray diffraction data demonstrated that, in the precipitate, the internal structure has a lamellar organization. There is no reason to doubt that the same organization prevails inside the dispersed aggregates. The repeat distance found from X-ray diffraction measurements was 37 Å, corroborating the data obtained by SANS. We note that similar repeat distances have been found in aggregates between linear polyvinylamine and SDS,[44] where a repeat distance of 36.1 Å was reported. Lower values were obtained by Zhou et al.,[45] when working with polyvinylamine and alkyl sulfates with different chain lengths ($n = 10$, 11, 14, and 16); the values reported in that work varied between 31.7 and 34 Å. They also concluded that for lower surfactant chain lengths the surfactant chains in the complexes were fully extended, while for the larger surfactant chains stronger hydrophobic interactions among the alkyl chains could lead to an overlapped or tilted arrangement due to the lack of space.[45]

In the present case it seems that the interlamellar separation is large enough to allow the surfactant chains to be arranged nearly fully extended and perpendicular to the lamellar surface.

It is interesting to note that the branched structure of PEI does not result in any large change in interlamellar spacing as compared to the linear polyvinylamine. This is consistent with the elongated and flat structure deduced for PEI alone, which readily would fit into the space between surfactant bilayers without requiring major conformational changes.

Conclusions

The combination of different scattering methods, static light scattering, dynamic light scattering, small-angle neutron scattering, and X-ray diffraction has provided a detailed picture of the structure of PEI/SDS aggregates. In alkaline solutions, at pD 10.1, the polyelectrolyte acts as a template for surfactant association. The polyelectrolyte chain does not undergo major conformational changes due to association with SDS, but rather remains in an elongated ellipsoidal form with a small thickness. Once a critical surfactant concentration has been reached the individual polyelectrolyte−surfactant complexes start to aggregate and stack on top of each other. The stacked structure is not very ordered but does give rise to a pronounced feature in the scattering curve. A decrease in pH results in a more pronounced association between PEI and SDS. The initial binding of SDS at pD 4.9 does not, just as at higher pH, result in any major changes in the polyelectrolyte conformation. As the surfactant association proceeds three-dimensional aggregates, involving several polyelectrolyte chains and SDS, are formed. The internal organization of these aggregates consists of surfactant bilayers separated by polyelectrolytes and water in a lamellar arrangement. Thus, by increasing the charge density of the polyelectrolyte, via decreasing the pD value, the stacked aggregates with poorly defined repeat distance are transformed into a highly organized lamellar structure.

References and Notes

(1) Water-Soluble Synthetic Polymers. In *Water-Soluble Synthetic Polymers*: *Properties and Behavior*; Molyneux, P., Ed.; CRC Press: Boca Ratón, FL, 1983; Vol. 1.

(2) Water-Soluble Synthetic Polymers. In *Water-Soluble Synthetic Polymers*: *Properties and Behavior*; Molyneux, P., Ed.; CRC Press: Boca Ratón, FL, 1984; Vol. 2.

(3) Madkour, T. M. Poly(ethylene imine). In *Polymer Data Handbook*; Mark, J. E., Ed.; Oxford University Press: New York, 1999.

(4) Mészáros, R.; Thompson, L.; Bos, M.; de Groot, P. *Langmuir* **2002**, *18*, 6164.

(5) Mészáros, R.; Thompson, L.; Bos, M.; Varga, I.; Gilányi, T. *Langmuir* **2003**, *19*, 609.

(6) Bystryak, S. M.; Winnik, M. A. *Langmuir* **1999**, *15*, 3748.

(7) Li, Y.; Ghoreishi, J.; Warr, J.; Bloor, D. M.; Holzwarth, J. F.; Wyn-Jones, E. *Langmuir* **2000**, *16*, 3093.

(8) Li, Y.; Xu, R.; Couderc, S.; Bloor, D. M.; Warr, J.; Penfold, J.; Holzwarth, J. F.; Wyn-Jones, E. *Langmuir* **2001**, *17*, 5657.

(9) Park, I. H.; Choi, E. *Polymer* **1996**, *37*, 313.

(10) Winnik, M. A.; Bystryak, S. M.; Chassenieux, C. *Langmuir* **2000**, *16*, 4495.

(11) Naderi, A.; Dedinaite, A.; Claesson, P. Colloids and surfaces A: Physicochemical and Engineering Aspects. Submitted for publication, 2004.

(12) Dedinaite, A.; Mészáros, R.; Claesson, P. *J. Phys. Chem. B* **2004**, *108*, 11645.

(13) Claesson, P. M.; Blomberg, E.; Paulson, O. E. H.; Malmsten, M. *Colloids Surf. A* **1996**, *112*, 131.

(14) Claesson, P. M.; Paulson, O. E. H.; Blomberg, E.; Burns, N. L. *Colloids Surf. A* **1997**, *123*−*124*.

(15) Poptoshev, E.; Claesson, P. *Langmuir* **2002**, *18*, 2590.

(16) Windsor, R.; Neivandt, D. J.; Davies, P. B. *Langmuir* **2001**, *17*, 7306.

(17) Bates, R. G. *Determination of pH*: *Theory and practice*, 1st ed.; John Wiley and Sons: New York, 1964.

(18) Glasoe, P. K.; Long, F. A. *J. Phys. Chem.* **1960**, *64*, 188.

(19) Krezel, A.; Bal, W. *J. Inorg. Biochem.* **2004**, *98*, 161.

(20) Bastardo, L.; Claesson, P.; Brown, W. *Langmuir* **2002**, *18*, 3848.

(21) Ericsson, C. A.; Söderman, O.; Garamus, V. M.; Bergström, M.; Ulvenlund, S. *Langmuir* **2004**, *20*, 1401.

(22) Koppel, D. E. *J. Chem. Phys.* **1972**, *57*, 4814.

(23) Borsali, R. Scattering properties of ternary polymer solutions. In *Light Scattering*: *Principles and Development*; Brown, W., Ed.; Clarendon Press: Oxford, 1996.

(24) Stuhrmann, H. B.; Burkhard, N.; Dietrich, G.; Jünemann, R.; Meerwinck, W.; Schmitt, M.; Wadzack, J.; Willumeit, R.; Zhao, J.; Nierhaus, K. H. *Nucl. Instrum. Methods Phys. Res., Sect. A* **1995**, *356*, 124.

(25) Cotton, J. P. Introduction to an Investigative Tool for Colloidal and Polymeric Systems. In *Neutron, X.-Ray and Light Scattering*; Lindner, P., Zemb, T., Eds.; North-Holland: Amsterdam, The Netherlands, 1991.

(26) Wignall, G. D.; Bates, F. S. *J. Appl. Crystallogr.* **1987**, *20*, 28.

(27) Hashida, T.; Tashiro, K.; Aoshima, S.; Inaki, Y. *Macromolecules* **2002**, *35*, 4330.

(28) *CRC Handbook of Chemistry and Physics*, 84th ed.; Lide, D. R., Ed.; CRC Press: Boca Raton, FL, 2004.

(29) Guinier, A. *X-ray Diffraction*; W. H. Freeman and Co.: San Francisco, CA, 1963.

(30) Pedersen, J. S.; Vyskocil, P.; Schönfeld, B.; Kostorz, G. *J. Appl. Crystallogr.* **1997**, *30*, 975.

(31) Bergström, M.; Pedersen, J. S.; Schurtenberger, P.; Egelhaaf, S. U. *J. Phys. Chem. B* **1999**, *103*, 9888.

(32) Pedersen, J. S. *J. Phys. IV* **1993**, *3*, 491.

(33) Pedersen, J. S.; Posselt, D.; Mortensen, K. *J. Appl. Crystallogr.***1990**, *23*, 321.

(34) Bevington, P. R. *Data reduction and error analysis for the physical sciences*; McGraw-Hill: New York, 1969.

(35) Evans, D. F.; Wennerstrom, H. *The Colloidal Domain*: *Where physics, Chemistry, Biology and Technology Meet*, 2nd ed.; Wiley-VCH: New York, 1999.

(36) Sedlák, M. Structure and Dynamics of Polyelectrolyte Solutions by light Scattering. In *Physical Chemistry of Polyelectrolytes*; Radeva, T., Ed.; Marcell Dekker: New York, 2001; Vol. 99.

(37) Sedlák, M. Polyelectrolytes in Solution. In *Light Scattering*: *Principles and Development*, 1st ed.; Brown, W., Ed.; Clarendon Press and Oxford Science Publications: New York, 1996; p 528.

(38) Bergström, L. M.; Kjellin, U. R. M.; Claesson, P. M.; Grillo, I. *J. Phys. Chem. B* **2004**, *108*, 1874.

(39) *Interactions of Surfactants with Polymers and Proteins*; Goddard, E. D., Ananthapadmanabhan, K. P., Eds.; CRC Press: Boca Raton, FL, 1993.

(40) Ilekti, P.; Picullel, L.; Tournilhac, F.; Cabane, B. *J. Phys. Chem. B* **1998**, *102*, 344.

(41) Dedinaite, A.; Claesson, P. M.; Nygren, J.; Iliopoulos, I. *Progr. Colloid Polym. Sci.* **2000**, *116*, 84.

(42) Claesson, P. M.; Bergström, M.; Dedinaite, A.; Kjellin, M.; Legrand, J.-F.; Grillo, I. *J. Phys. Chem. B* **2000**, *104*, 11689.

(43) Bergström, M.; Pedersen, J. S. *Phys. Chem. Chem. Phys.* **1999**, *1*, 4437.

(44) Bergström, M.; Kjellin, U. R. M.; Claesson, P. M.; Pedersen, J. S.; Nielsen, M. M. *J. Phys. Chem. B* **2002**, *106*, 11412.

(45) Zhou, S.; Hu, H.; Burger, C.; Chu, B. *Macromolecules* **2001**, *34*, 1772.

(46) Chu, B. *Laser Light Scattering*; Academic Press: New York, 1974.

(47) King, S. Small-angle Neutron Scattering. In *Modern Techniques for Polymer Characterization*; Pethrick, R. A., Dawkins, J. V., Eds.; John Wiley & Sons Ltd: Chichester, UK, 1999; p 171.